Data Sheet (Cat.No.T1661)

TargetMol

Crizotinib

Chemical Properties

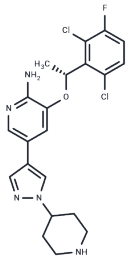

CAS No. : 877399-52-5

Formula: C21H22Cl2FN5O

Molecular Weight: 450.34

Storage: Powder: -20°C for 3 years | In solvent: -80°C for 1 year
Actual storage temperature shall be subject to the COA.

Biological Description

Description	Crizotinib (PF-02341066) is an ATP-competitive small-molecule tyrosine kinase inhibitor of c-MET (IC50: 8 nM) and ALK (IC50: 20 nM) receptors.
Targets(IC50)	ALK,Autophagy,c-Met/HGFR,ROS,ROS Kinase
In vitro	Crizotinib (PF-2341066) potently inhibited c-Met phosphorylation and c-Met-dependent proliferation, migration, or invasion of human tumor cells in vitro (IC50: 5-20 nmol/L). In addition, PF-2341066 potently inhibited HGF-stimulated endothelial cell survival or invasion and serum-stimulated tubulogenesis in vitro [1]. Both of two cell lines with MET amplification, EBC-1, and H1993, were sensitive to crizotinib (IC50: 10 nM). In contrast, crizotinib did not substantially inhibit the proliferation of lung cancer cells with a MET mutation (H2122, H1437, and H596) [2]. PF-2341066 potently inhibited NPM-ALK phosphorylation in Karpas299 or SU-DHL-1 ALCL cells (IC50: 24 nmol/L). PF-2341066 potently inhibited cell proliferation, which was associated with G(1)-S-phase cell cycle arrest and induction of apoptosis in ALK-positive ALCL cells (IC50: 30 nmol/L) but not ALK-negative lymphoma cells. The induction of apoptosis was confirmed using terminal deoxyribonucleotide transferase-mediated nick-end labeling and Annexin V staining (IC50: 25-50 nmol/L) [3].
In vivo	PF-2341066 showed efficacy at well-tolerated doses, including marked cytoreductive antitumor activity, in several tumor models that expressed activated c-Met. The antitumor efficacy of PF-2341066 was dose-dependent and showed a strong correlation to the inhibition of c-Met phosphorylation in vivo. Near-maximal inhibition of c-Met activity for the full dosing interval was necessary to maximize the efficacy of PF-2341066. Additional mechanism-of-action studies showed a dose-dependent inhibition of c-Met-dependent signal transduction, tumor cell proliferation (Ki67), induction of apoptosis (caspase-3), and reduction of microvessel density (CD31) [1]. Treatment of c-MET-amplified GTL-16 xenografts with 50 mg/kg crizotinib caused tumor regression that was associated with a slow reduction in (18)F-FDG uptake and reduced expression of the GLUT-1. Although baseline (18)F-FDG uptake into U87MG tumors was substantially higher than in GTL-16 tumors, (18)F-FDG uptake into U87MG tumors remained unchanged on treatment at 50 mg/kg crizotinib, despite tumor growth inhibition of 93% on day 8 of treatment [4].
Kinase Assay	c-Met catalytic activity was quantitated using a continuous-coupled spectrophotometric assay in which the time-dependent production of ADP by c-Met was determined by

Kinase Assay	analysis of the rate of consumption of NADH. NADH consumption was measured by a decrease in absorbance at 340 nm by spectrophotometry at designated time points. To determine Ki values, PF-2341066 was introduced into test wells at various concentrations in the presence of assay reagents and incubated for 10 min at 37°C. The assay was initiated by the addition of the c-Met enzyme [1].
Cell Research	Cells were seeded in 96-well plates in media supplemented with 10% fetal bovine serum (FBS) and transferred to serum-free media (with 0.04% BSA) after 24 h. In experiments investigating ligand-dependent RTK phosphorylation, corresponding growth factors were added for up to 20 min. After incubation of cells with PF-2341066 for 1 h and/or appropriate ligands for the designated times, cells were washed once with HBSS supplemented with 1 mmol/L Na3VO4, and protein lysates were generated from cells. Subsequently, phosphorylation of selected protein kinases was assessed by a sandwich ELISA method using specific capture antibodies used to coat 96-well plates and a detection antibody specific for phosphorylated tyrosine residues. Antibody-coated plates were (a) incubated in the presence of protein lysates at 4°C overnight; (b) washed seven times in 1% Tween 20 in PBS; (c) incubated in a horseradish peroxidase-conjugated anti-total-phosphotyrosine (PY-20) antibody (1:500) for 30 min; (d) washed seven times again; (e) incubated in 3,3′,5,5′-tetramethylbenzidine peroxidase substrate to initiate a colorimetric reaction that was stopped by adding 0.09 N H2SO4; and (f) measured for absorbance in 450 nm using a spectrophotometer [1].
Animal Research	Daily treatment with PF-2341066 given in water by oral gavage was initiated when tumors were 100 to 600 mm^3 in volume. Tumor volume was determined by measurement with electronic Vernier calipers, and tumor volume was calculated as the product of its length × width2 × 0.4. Tumor volume was expressed on indicated days as the median tumor volume ± SE indicated for groups of mice. Percent (%) inhibition values were measured on the final day of study for drug-treated compared with vehicle-treated mice and are calculated as 100 × {1?[(TreatedFinal day ? TreatedDay 1)/ (ControlFinal day ? ControlDay 1)]}. Tumor regression values were determined by calculating the ratio of median tumor volumes at the time when treatment was initiated to the median tumor volume on the final day of study for a given treatment group. Significant differences between the treated versus the control groups (P ≤ 0.001) were determined using one-way ANOVA [1].

Solubility Information

Solubility	DMSO: 34.5 mg/mL (76.61 mM),Sonication and heating are recommended. (< 1 mg/ml refers to the product slightly soluble or insoluble)
In vivo Formulation	10% DMSO+90% Saline: 1 mg/mL (2.22 mM),Solution. *Please add the solvents sequentially, clarifying the solution as much as possible before adding the next one. Dissolve by heating and/or sonication if necessary. Working solution is recommended to be prepared and used immediately. The formulation provided above is for reference purposes only. In vivo formulations may vary and should be modified based on specific experimental conditions.*

Preparing Stock Solutions

	1mg	5mg	10mg
1 mM	2.2205 mL	11.1027 mL	22.2054 mL
5 mM	0.4441 mL	2.2205 mL	4.4411 mL
10 mM	0.2221 mL	1.1103 mL	2.2205 mL
50 mM	0.0444 mL	0.2221 mL	0.4441 mL

Please select the appropriate solvent to prepare the stock solution, according to the solubility of the product in different solvents. Please use it as soon as possible.

Note: The dilution table applies only to solid products. For liquid products, please calculate the stock solution based on the stated concentration and/or density.

Reference

Zou HY, et al. An orally available small-molecule inhibitor of c-Met, PF-2341066, exhibits cytoreductive antitumor efficacy through antiproliferative and antiangiogenic mechanisms. Cancer Res. 2007 May 1;67(9):4408-17.
Yan H, Wu W, Hu Y, et al.Regorafenib inhibits EphA2 phosphorylation and leads to liver damage via the ERK/MDM2/p53 axis.Nature Communications.2023, 14(1): 2756.
Zheng Y D, Zhong T, Wu H, et al. Crizotinib Shows Antibacterial Activity against Gram-Positive Bacteria by Reducing ATP Production and Targeting the CTP Synthase PyrG. Microbiology Spectrum. 2022: e00884-22
Kastana P, Ntenekou D, Mourkogianni E, et al.Genetic deletion or tyrosine phosphatase inhibition of PTPRZ1 activates c-Met to up-regulate angiogenesis and lung adenocarcinoma growth.International Journal of Cancer.. 2023;1-16.
Wu W, Li J, Yin Y, et al.Rutin attenuates ensartinib-induced hepatotoxicity by non-transcriptional regulation of TXNIP.Cell Biology and Toxicology.2024, 40(1): 38.
Liu Z, Zhang Y, Zhuang H, et al.Inhibiting the Otub1/phosphorylated STAT3 axis for the treatment of non-small cell lung cancer.Acta Pharmacologica Sinica.2024: 1-12.
Mourkogianni E, Karavasili K, Xanthopoulos A, et al.Pleiotrophin Activates cMet-and mTORC1-Dependent Protein Synthesis through PTPRZ1—The Role of αvβ3 Integrin.International Journal of Molecular Sciences.2024, 25(19): 10839.
Yang W H, Huang B Y, Rao H Y, et al.Ribonuclease 1 Induces T-Cell Dysfunction and Impairs CD8+ T-Cell Cytotoxicity to Benefit Tumor Growth through Hijacking STAT1.Advanced Science.2025: 2404961.
Yan H, Huang X, Zhou Y, et al.Disturbing Cholesterol/Sphingolipid Metabolism by Squalene Epoxidase Arises Crizotinib Hepatotoxicity.Advanced Science.2025: 2414923.
Li P, Jia C, Fan Z, et al.Discovery of novel exceptionally potent and orally active c-MET PROTACs for the treatment of tumors with MET alterations.Acta Pharmaceutica Sinica B.2023
Tanizaki J, et al. MET tyrosine kinase inhibitor crizotinib (PF-02341066) shows differential antitumor effects in non-small cell lung cancer according to MET alterations. J Thorac Oncol. 2011 Oct;6(10):1624-31.
Christensen JG, et al. Cytoreductive antitumor activity of PF-2341066, a novel inhibitor of anaplastic lymphoma kinase and c-Met, in experimental models of anaplastic large-cell lymphoma. Mol Cancer Ther. 2007, 6(12 Pt 1), 3314-3322.
Zou X, Zeng M, Zheng Y, et al.Comparative Study of Hydroxytyrosol Acetate and Hydroxytyrosol in Activating Phase II Enzymes.Antioxidants.2023, 12(10): 1834.
Cullinane C, et al. Differential (18)F-FDG and 3'-deoxy-3'-(18)F-fluorothymidine PET responses to pharmacologic inhibition of the c-MET receptor in preclinical tumor models. J Nucl Med. 2011 Aug;52(8):1261-7
Jiao D, Chen Y, Liu X, et al.Targeting MET endocytosis or degradation to overcome HGF-induced gefitinib resistance in EGFR-sensitive mutant lung adenocarcinoma.Biochemical and Biophysical Research Communications.2023
Yu J, Zhang L, Peng J, et al. Dictamnine, a novel c-Met inhibitor, suppresses the proliferation of lung cancer cells by downregulating the PI3K/AKT/mTOR and MAPK signaling pathways. Biochemical pharmacology. 2022, 195: 114864.
Arechederra M, Bazai S K, Abdouni A, et al. ADAMTSL5 is an epigenetically activated gene underlying tumorigenesis and drug resistance in hepatocellular carcinoma. Journal of Hepatology. 2021, 74(4): 893-906.
Tucker ER, et al. Immunoassays for the quantification of ALK and phosphorylated ALK support the evaluation of on-target ALK inhibitors in neuroblastoma. Mol Oncol. 2017 Aug;11(8):996-1006.
Yang Y, Huang J, Xie N, et al. lincROR influences the stemness and crizotinib resistance in eMl-alK+ non-small-cell lung cancer cells[J]. OncoTargets and therapy. 2018 Jun 22;11:3649-3657.
Yang Y, Huang J, Xie N, et al. lincROR influences the stemness and crizotinib resistance in eMl-alK+ non-small-cell lung cancer cells. OncoTargets and Therapy. 2018 Jun 22;11:3649-3657
Hu Y, Zhang X, Zhao Z, et al. Keratinocytes apoptosis contributes to crizotinib induced-erythroderma[J]. Toxicology Letters. 2019
Tao J, Tu Y, Liu P, et al. Detection of colorectal cancer using a small molecular fluorescent probe targeted against c-Met. Talanta. 2021: 122128.
Tao J, Tu Y, Liu P, et al. Detection of colorectal cancer using a small molecular fluorescent probe targeted against c-Met[J]. Talanta. 2021: 122128.
Hu Y, Zhang X, Zhao Z, et al. Keratinocytes apoptosis contributes to crizotinib induced-erythroderma. Toxicology

Letters. 2019